Design of a Special Lead Extrusion Damper

C.Soydan, A.Gullu, O.E.Hepbostancı
Graduate School of Istanbul Technical University, Istanbul, Turkey

E.Yuksel
Istanbul Technical University Faculty of Civil Engineering, Istanbul, Turkey

E.Irtem
Balıkesir University, Department of Civil Engineering, Balıkesir, Turkey

SUMMARY:
Earthquake ground motions impart significant amount of energy into the structures. The modern structural design seeks to absorb an amount of this energy through the energy dissipater elements that are located to special locations within the structures. An experimental study has been initiated to design more efficient lead extrusion dampers (LED) as a subject of the first author's Ph.D thesis. Early results of the study are presented here. Load-displacement relationships are obtained for several LEDs which are placed on a specially designed testing setup. The recurrent sinusoidal displacement cycles having altered frequency and amplitude thresholds are used in the study. The effects of frequency and amplitude variables on the energy dissipation, damping and stiffness characteristics of the improved LED are investigated. Furthermore, the number of cycles used in the loading pattern is one of the other imperative parameter to define the nominal damping characteristic of the improved LED.

Keywords: Lead extrusion damper, Passive control systems, Energy dissipation

1. INTRODUCTION

Passive energy dissipation device play a role similar to that of seismic isolators namely to absorb and dissipate a significant portion of the energy input to a building by earthquake shaking. Energy dissipation devices are typically distributed throughout a structure to absorb either kinetic or strain energy transmitted from the ground into the primary system (Aiken, 1996). Damping in structures can significantly reduce the displacement and acceleration responses, and decrease the shear forces, along the height of buildings. Energy dissipation in buildings can be confined mainly to supplemental dampers. Damage to the building can be limited to supplemental dampers which are easier to replace than structural components (Sadek et al., 1996).

Research and development in both the academic and industrial arenas over the past decade has advanced both the concepts and the hardware of supplemental damping to the point where a number of different passive dissipation solutions with varying hysteretic characteristics are available. Of course the suitability of a particular device for a given application depends on the requirements of the designer. Factors such as the allowed force to be transferred to the structural members adjacent to the device, the expected relative displacements across the device connection points, and the required amount of energy to be dissipated must be all considered (Aiken, 1996).

The LED that is used within this study is a passive energy dissipation device. The energy dissipation is occurred with the plastic deformation of lead existing in the LED. A loading frame has been set up in Istanbul Technical University Structural and Earthquake Engineering Laboratory (STEELAB) on which different types of LEDs with various dimensions can be mounted. A ±33 mm displacement capacity LED has been designed and manufactured in this study and the force-displacement relationships are obtained under the excitation of sinusoidal displacement cycles having altered frequency and amplitude thresholds. The effects of frequency and amplitude variables on the energy

dissipation, damping and stiffness characteristics of the improved LED are investigated.

2. LEAD EXTRUSION DAMPERS

LED utilizes the hysteretic energy dissipation properties of lead. The process of extrusion consists of forcing a material through a hole or an orifice, thereby altering its shape (Sadek et al., 1996). The pressure applied to the ram forces the lead to flow through the orifice, producing a microstructure of elongated grains containing many crystal lattice defects. A proportion of the energy required to extrude the lead appears immediately as heat, but some is stored in the deformed lead and is the primary driving force for three interrelated processes (recovery, recrystallization and gain growth) which tend to restore the lead to its original condition (Wulf et al., 1953; Birchenall, 1959) (Fig. 2.1).

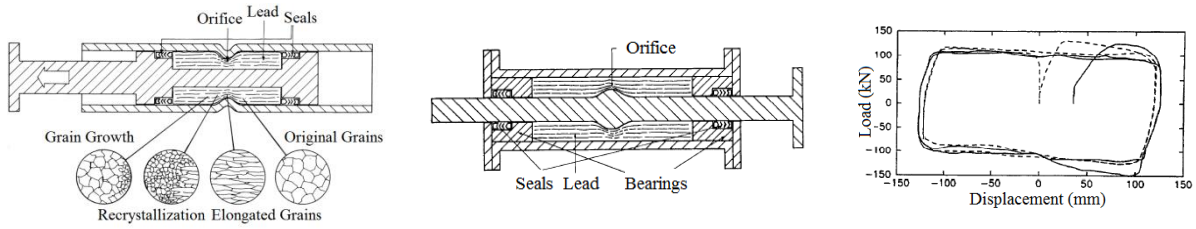

(a) (b) (c)

Figure 2.1. LED; (a) Longitudinal section of a constricted tube LED showing the changes in microstructure of the lead (Robinson and Greenbank, 1975) (b) Longitudinal section of a bulged shaft LED (Robinson and Greenbank, 1976) (c) Hysteresis loops of LED (Robinson and Cousins, 1987)

Essentially the LED consists of a thick-walled tube having a construction, on either side of which are two pistons are connected by a tie rod. The space between the pistons is filled with lead, which is separated from the cylinder wall by a thin layer of lubricant kept in place by hydraulic seals around the pistons. One piston is effectively part of a connecting rod which extends beyond one end of cylinder and is fixed to the structure, while the opposite end of the cylinder is fixed to another part of the structure. When the two parts of the structure oscillate relative to each other (as during an earthquake) the lead is extruded back and forth through the orifice. Since extrusion is a process of plastic deformation, work must be done as the pistons move relative to the cylinder. Thus in an earthquake protection application such a device would limit the build-up of destructive oscillations in the structure (Robinson and Greenbank, 1975).

According to Skinner et al. (1993), LED's were first suggested by Robinson as a passive energy dissipation device for base isolated structures in New Zealand. Two devices introduced by Robinson are shown in Fig. 2.1 (Robinson and Greenbank, 1975, 1976). The first device consists of a thick-walled tube and co-axial shaft with a piston (Fig. 2.1.a). The second device is similar to the first device except that the extrusion orifice is formed by a bulge on the central shaft rather than by a constriction in the tube. The shaft is supported by bearings which also serve to hold the lead in place. As the shaft moves, the lead must extrude through the orifice formed by the bulge and tube (Fig 2.1.b). The hysteretic behaviour of LEDs is essentially rectangular (Fig. 2.1.c) (Sadek et al., 1996)

3. EXPERIMENTAL STUDY

An experimental setup is used to obtain the force-displacement relationships of the designed LED. Loading frame, adaptor elements and out-of-plane systems have been deliberated and constructed within this experimental study. The loading frame has been installed into an existing frame and the experimental studies has been started to investigate the rigidity and damping properties of LED (Fig. 3.1).

Figure 3.1. Loading frame and experimental setup

3.1. LED

A bulged shaft LED design is adopted in this study. LED consists of three parts which are the shaft, the tube and the cap. There is a sphere shaped bulge at the centre of the shaft. The space between the elements is filled with lead. The diameter of the shaft and the bulge are 32 mm and 44 mm, respectively. The internal diameter of the tube is 60 mm and the thickness of the tube is 12 mm. The gap between the bulge and the tube is 8 mm. The displacement capacity of the LED is ±33 mm (Fig. 3.2).

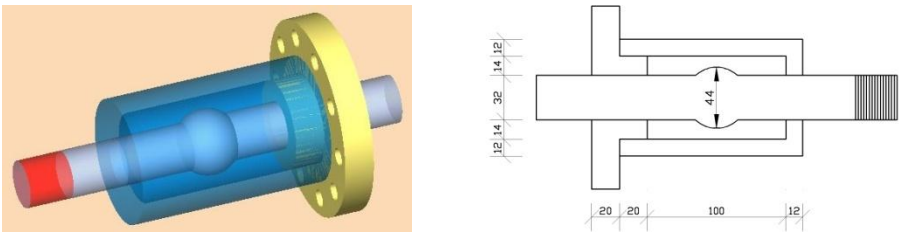

Figure 3.2. 3D demonstration and dimensions of LED

In this study, the layer of lubricant is not used between the lead and the tube wall which is distinct from Robinson and Greenbank (1975, 1976) and Cousins and Porritt (1993). Therefore, there is no need for hydraulic seals that is used for the lubricant to be kept in place. The device lubrication was not found to be necessary in the studies that have been done by Rodgers et. al. (2006) and Rodgers (2009) either. The tube and the cap are designed as bearings in order to locate the shaft, to maintain the axial back and forth movement of the shaft and to hold the lead in place. This design prevents the LED from having additional bearings. Robinson and Greenbank (1975, 1976), Cousins and Porritt (1993) and Tsai, Lai, Chang, Li (2002) didn't mention about prestressing of lead. In the studies performed by Rodgers et al. (2006), Rodgers et al. (2006) and Rodgers (2009), the lead is prestressed to minimize the void formation and the effect of prestressing on the behaviour of LED is investigated. In this study, the cap of the LED has a special cross section with two different thicknesses, so the prestressing on the lead is realized with the assembly of the cap on the LED (Fig. 3.2).

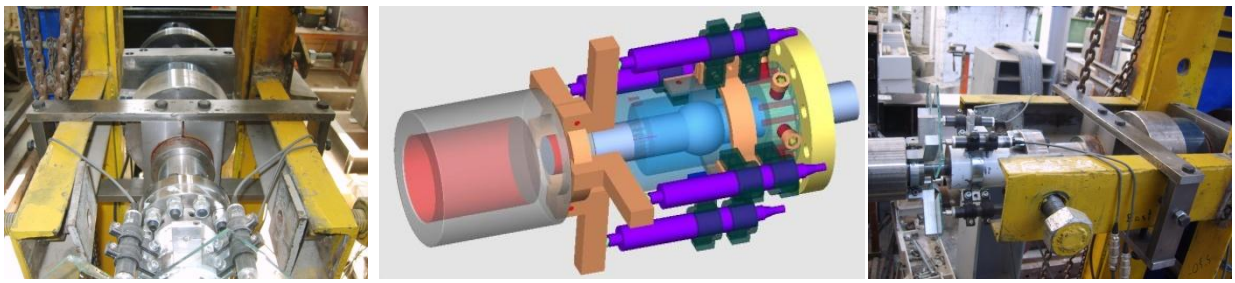

Figure 3.3. Out-of-plane restraints and LED displacement monitoring

3.2. Loading Frame

A concentrically braced loading setup consist of two planar frames has been constructed (Fig. 3.1). The loading setup has high lateral stiffness and load capacity to be used in the tests of different types of LEDs. The loading setup is installed in an existing loading frame in the laboratory. Actuator is kept in the horizontal alignment by means of the out of plane retainers (Fig. 3.3).

3.3. Experimental Setup

Experimental setup consists of various capacities of transducers and a load cell having a capacity of 300 kN which has been used for monitoring the LED's restoring force. The displacement of the LED has been monitored with four transducers located radially around the LED. These transducers have been installed on the LED via a clamp with a plane against of the transducers in order to monitor the relative displacement of the shaft (Fig. 3.3). The data taken from these four transducers remain close each other during the tests so the average of the data is considered as the displacement of LED. Ten transducers have been used in various locations to monitor in-plane and out of plane movements of the loading frames. The measurements exposed that the out of plane and rigid body movements are negligible compared with the relative displacements of LED.

3.4. Constant Frequency Altered Amplitude

The data collection capability of the static data logger used in this study has been considered to determine the period of sinusoidal displacement excitation. The period is identified as 60 seconds and each run consists of 30 cycles. Four tests have been carried out with a constant frequency of 0.01667 Hz and the average displacements of LED are 2.75 mm, 3.58 mm, 4.00 mm and 4.47 mm, respectively (Fig. 3.4).

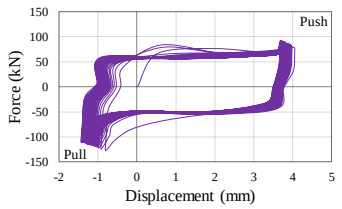

(a) u_o = 2.75 mm

Maximum
P_{push}=91.9 kN
P_{pull}=126.8 kN

u_{push}=4.05 mm
u_{pull}=1.45 mm

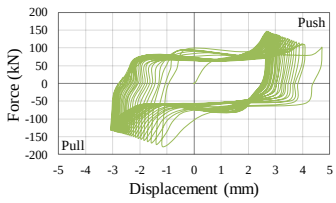

(b) u_o = 3.58 mm

Maximum
P_{push}=147.0 kN
P_{pull}=178.1 kN

u_{push}=4.71 mm
u_{pull}=3.07 mm

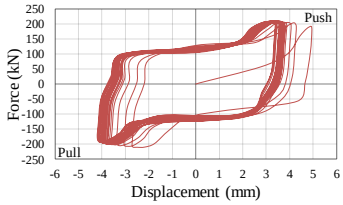

(c) u_o = 4.00 mm

Maximum
P_{push}=209.7 kN
P_{pull}=209.9 kN

u_{push}=4.96 mm
u_{pull}=4.21 mm

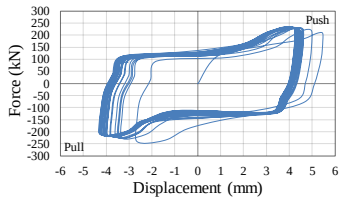

(d) u_o = 4.47 mm

Maximum
P_{push}=233.9 kN
P_{pull}=247.0 kN

u_{push}=5.47 mm
u_{pull}=4.31 mm

Figure 3.4. Force-displacement relationships (f = 0.01667 Hz)

The general shape of the force-displacement relationships is very similar. The force-displacement relationship of the first case isn't symmetrical with respect to the origin but the loops remain almost the same during 30 cycles (Fig. 3.4.a). For the second case, where the response displacement amplitude is 3.58 mm, the force-displacement relationship isn't symmetrical at first cycles but the loops are symmetrical and approximately the same for the last ten cycles (Fig. 3.4.b). The force-displacement relationship for the third and the last case the loops are stable and remain almost the same after a few cycle (Fig. 3.4.c, Fig 3.4.d). The force-displacement relationship of the third case has a different path at the beginning of the first cycle distinct from the other cases.

3.5. Constant Amplitude Altered Frequency

The dynamic data logger used in this part of the study has a capability of 2.5 kHz frequency response. Nine tests have been carried out with constant displacement amplitude of 2 mm for the LED and the frequencies of 1.0 Hz-0.2 Hz with steps of 0.1 Hz. The purpose of the frequency tests is to determine the effect of the frequency of excitation on the behaviour of LED. Each set of tests consists of 5 cycles.

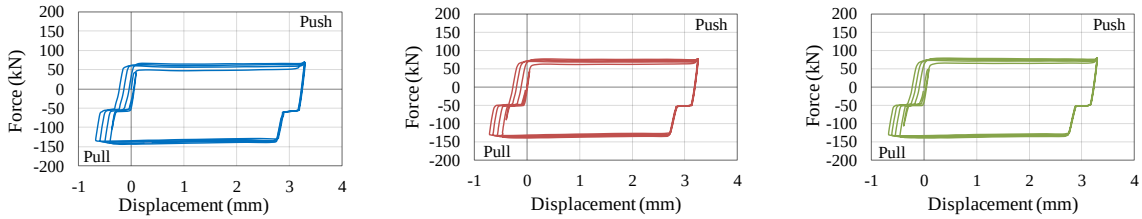

f=1 Hz u_o=1.990 mm
P_{push}=69.5 kN P_{pull}=143.8 kN
u_{push}=3.03 mm u_{pull}=0.68 mm

f=0.9 Hz u_o=1.984 mm
P_{push}=76.7 kN P_{pull}=139.6 kN
u_{push}=3.26 mm u_{pull}=0.71 mm

f=0.8 Hz u_o=1.985 mm
P_{push}=80.3 kN P_{pull}=139.4 kN
u_{push}=3.29 mm u_{pull}=0.68 mm

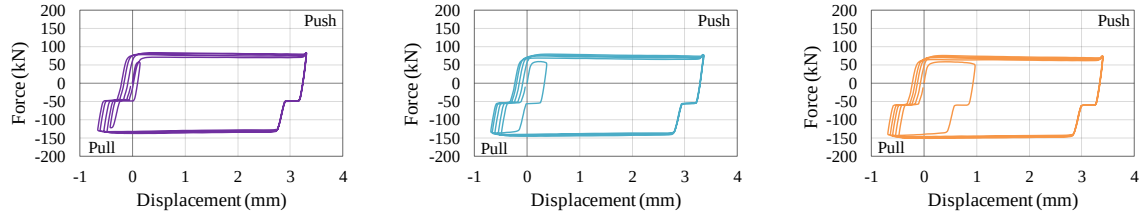

f=0.7 Hz u_o=1.984 mm
P_{push}=83.4 kN P_{pull}=138.7 kN
u_{push}=3.31 mm u_{pull}=0.68 mm

f=0.6 Hz u_o=2.025 mm
P_{push}=79.5 kN P_{pull}=145.4 kN
u_{push}=3.36 mm u_{pull}=0.69 mm

f=0.5 Hz u_o=2.043 mm
P_{push}=75.1 kN P_{pull}=151.6 kN
u_{push}=3.40 mm u_{pull}=0.68 mm

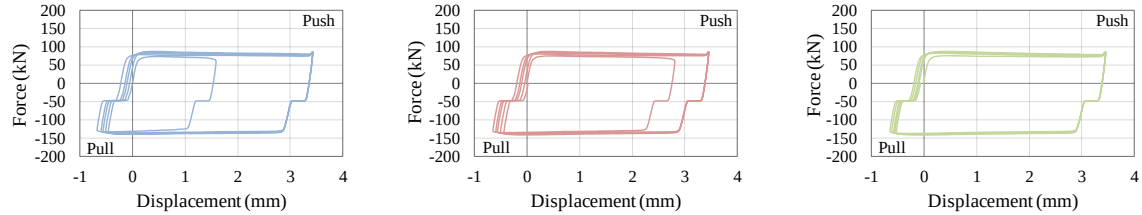

f=0.4 Hz u_o=2.057 mm
P_{push}=87.0 kN P_{pull}=140.9 kN
u_{push}=3.44 mm u_{pull}=0.68 mm

f=0.3 Hz u_o=2.051 mm
P_{push}=87.7 kN P_{pull}=142.2 kN
u_{push}=3.45 mm u_{pull}=0.65 mm

f=0.2 Hz u_o=2.053 mm
P_{push}=87.8 kN P_{pull}=142.0 kN
u_{push}=3.46 mm u_{pull}=0.64 mm

Figure 3.5. Force-displacement relationships (u_o≈2 mm)

The difference between the relationships was resulted from the formation of the first cycle. The force-displacement relationships are almost the same for all frequency levels after first cycle.

4. ENERGY DISSIPATION

After the discretization of the hysteresis loops which have been obtained from the constant frequency-altered amplitude and the constant amplitude-altered frequency studies, the dissipated energy have been determined by the calculation of the area enclosed by the hysteresis loop for each cycle.

4.1. Constant Frequency Altered Amplitude

The dissipated energy that has been determined for the altered displacement amplitudes are given in Table 4.1. As the displacement amplitude increases the dissipated energy increase for the constant frequency (Fig. 4.1.a).

Table 4.1. Dissipated Energy (f = 0.01667 Hz)

u_o (mm)	Cycle	Min. (kNmm)	Max. (kNmm)	Total (kNmm)	Average (kNmm)
2.75	30	499	554	15439	515
3.58	30	324	882	21454	715
4.00	30	1076	1748	50222	1674
4.47	30	1918	2367	65924	2198

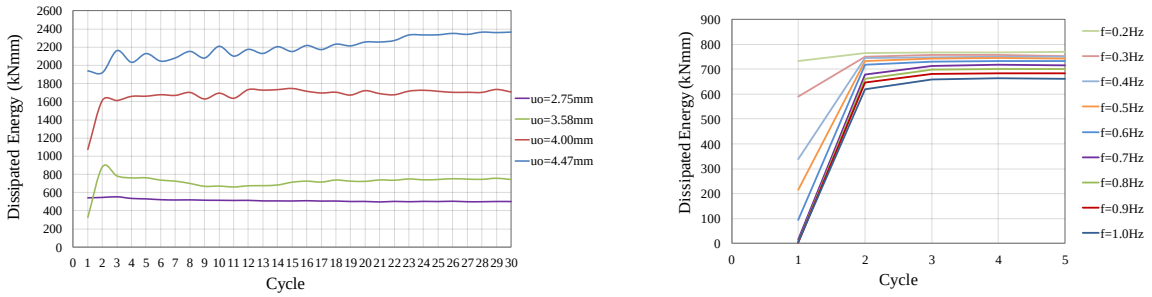

(a) f = 0.01667 Hz (b) $u_o \approx 2$ mm

Figure 4.1. Dissipated energy

4.2. Constant Amplitude Altered Frequency

The first cycle has not been considered in determining dissipated energy because of the difference between the force-displacement relationships was resulted from the formation of the first cycle. The dissipated energy increases min 1 % and max 8 % with respect to the dissipated energy in the second cycle for varying frequency levels (Table 4.2, Fig. 4.1.b). The dissipated energy remains almost the same as frequency decreases.

Table 4.2. Dissipated Energy ($u_o \approx 2$ mm)

f (Hz)	Cycle	Min. (kNmm)	Max.(kNmm)	Total (kNmm)	Average (kNmm)
1.0	4	619	659	2602	651
0.9	4	645	684	2695	674
0.8	4	661	701	2760	690
0.7	4	677	718	2822	706
0.6	4	718	734	2915	729
0.5	4	732	745	2963	741
0.4	4	744	751	2992	748
0.3	4	750	757	3016	754
0.2	4	765	769	3069	767

5. DETERMINATION OF MECHANICAL PROPERTIES

The analytical method used by Constantinou and Symans (1992) and Seleemah and Constantinou (1997) has been adopted for the determination of the mechanical properties of the LED.

5.1. General Equations

The actuator was run under displacement control such that the resulting motion of the damper shaft was sinusoidal. The damper motion is given by

$$u = u_o sin(\omega t) \tag{5.1}$$

where u_o is the amplitude of the displacement, ω is the frequency of motion and t is the time. For steady state conditions the force needed to maintain this motion is

$$P = P_o sin(\omega t + \delta) \tag{5.2}$$

where P_o is the amplitude of the force and δ is the phase angle. The area within the recorded force-displacement loops are measured to determine the energy dissipated in a single cycle of motion

$$W_d = \int P\, du \tag{5.3}$$

An equivalent ellipse that has the same energy dissipation can be defined as

$$W_d = \pi P_o u_o \sin(\delta) \tag{5.4}$$

Rewriting Equation 5.2,

$$P = P_o sin(\omega t) cos(\delta) + P_o cos(\omega t) sin(\delta) \tag{5.5}$$

And introducing the quantities

$$K_1 = (P_o/u_o) cos(\delta) \tag{5.6}$$

$$K_2 = (P_o/u_o) sin(\delta) \tag{5.7}$$

where K_1 is the storage stiffness and K_2 is the loss stiffness, one obtains

$$P = K_1 u_o sin(\omega t) + K_2 u_o cos(\omega t) \tag{5.8}$$

Equation 5.8 may also be written the form

$$P = K_1 u + (K_2/\omega)\dot{u} \tag{5.9}$$

where it is clear that first term represents the restoring force due to the stiffness of the damper which is in-phase with the displacement. The second term represents the force due to the damping of the damper which is in the phase with the velocity. Thus, the damping coefficient C of the damper is given by

$$C = K_2/\omega \tag{5.10}$$

Equations 5.4, 5.6 and 5.7 can be combined to give

$$\delta = sin^{-1}\left(\frac{K_2 u_o}{P_o}\right) \tag{5.11}$$

and

$$K_2 = \frac{W_d}{\pi u_o^2} \tag{5.12}$$

Equations 5.6, 5.7 and 5.10 through 5.12 can be used to obtain the mechanical properties of the damper from experimentally measured values of W_d, P_o and u_o.

In free vibration tests or tests carried out with static and dynamic loading, it is possible to determine damping with the energy relations. A force-deformation loop that is obtained from a cyclic excitation with the displacement amplitude u_o is shown in Fig. 5.1. The energy dissipated is given by the area E_D enclosed by the hysteresis loop and E_{So} is the maximum strain energy. Equivalent damping ratio which is expressed with Equation 5.13, can be obtained by equalizing the maximum strain energy with the

energy dissipated by viscous damping (Chopra, 2001). The dissipated energy and the maximum strain energy have been determined for each cycle in order to examine the experimental results by means of equivalent damping ratio.

$$\xi_{eq} = \frac{1}{4\pi}\frac{E_D}{E_{So}} \tag{5.13}$$

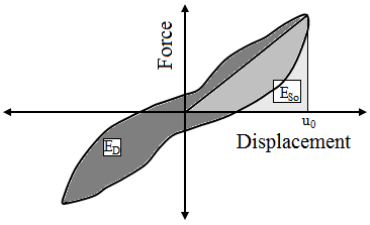

Şekil 5.1. Energy rate method (Chopra, 2001)

A computer code has been developed for usage of these equations. The mechanical properties of the LED have been determined with using this computer code.

5.2. Constant Frequency Altered Amplitude

The storage stiffness, the loss stiffness, the damping coefficient and the equivalent damping ratio is determined by the analytical method that is briefly explained in Section 5.1. The mechanical properties and the equivalent damping ratio of the LED remain nearly constant for the frequency of 0.01667 Hz after first few cycles (Fig. 5.2).

The storage stiffness varies between 32 kN/mm and 46 kN/mm generally. It changes from 32 kN/mm to 34 kN/mm for the 2.75 mm average displacement amplitude. The storage stiffness is determined as 44 kN/mm and 39 kN/mm for the first two cycles of the 3.58 mm average displacement amplitude. After the third cycle it varies between 40 kN/mm and 42 kN/mm. The storage stiffness decreases from 45 kN/mm to 38 kNmm for the first two cycles of the 4.00 mm average displacement amplitude. After the third cycle it changes from 36 kN/mm to 38 kN/mm. For the 4.47 mm average displacement amplitude the storage stiffness is determined as 41 kN/mm for the first cycle and decreases to 35 kN/mm at the end of 30 cycles.

The loss stiffness varies between 8 kN/mm and 37 kN/mm generally. It changes from 21 kN/mm to 24 kN/mm for the 2.75 mm average displacement amplitude. The loss stiffness is determined as 8 kN/mm and 22 kN/mm for the first two cycles of the 3.58 mm average displacement amplitude. After the third cycle it varies between 17 kN/mm and 20 kN/mm. The loss stiffness is determined as 22 kN/mm for the first cycle of the 4.00 mm average displacement amplitude. After the second cycle it changes from 32 kN/mm to 35 kN/mm. For the 4.47 mm average displacement amplitude the loss stiffness is determined as 31 kN/mm for the first cycle and increases to 37 kN/mm at the last cycle.

The damping coefficient varies between 75 kNs/mm and 350 kNs/mm generally. It changes from 200 kN/mm to 225 kNs/mm for the 2.75 mm average displacement amplitude. The damping coefficient is determined as 75 kNs/mm and 210 kNs/mm for the first two cycles of the 3.58 mm average displacement amplitude. After the third cycle it varies between 150 kNs/mm and 200 kNs/mm. The damping coefficient is determined as 210 kNs/mm for the first cycle of the 4.00 mm average displacement amplitude. After the second cycle it changes from 310 kN/mm to 330 kN/mm. For the 4.47 mm average displacement amplitude the damping coefficient is determined as 290 kN/mm for the first cycle and increases to 350 kN/mm at the end of 30 cycles.

The equivalent damping ratio varies between 0.08 and 0.37 generally. It changes from 0.27 to 0.30 for the 2.75 mm average displacement amplitude. The equivalent damping ratio is determined as 0.08 and 0.25 for the first two cycles of the 3.58 mm average displacement amplitude. After the third cycle it

varies between 0.18 and 0.22. The equivalent damping ratio is determined as 0.22 for the first cycle of the 4.00 mm average displacement amplitude. After the second cycle it changes from 0.32 to 0.35. For the 4.47 mm average displacement amplitude the equivalent damping ratio is determined as 0.30 for the first cycle and increases to 0.37 at the last cycle.

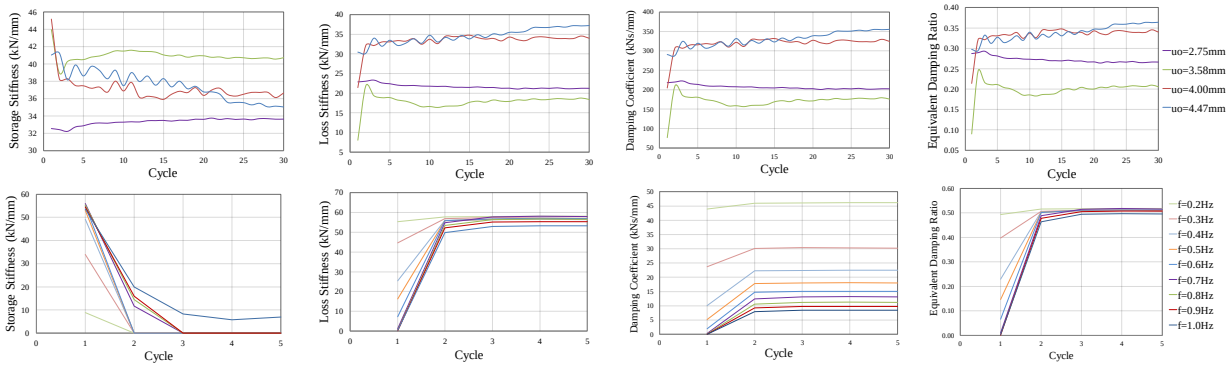

Figure 5.2. LED mechanical properties

5.3. Constant Amplitude Altered Frequency

The mechanical properties and the equivalent damping ratio are determined for the frequencies of 1.0 Hz-0.2 Hz with steps of 0.1 Hz (Fig. 5.2).

The storage stiffness is approximately 50 kN/mm between 0.4 Hz and 1 Hz in the first cycle. For 0.3 Hz and 0.2 Hz it is 34 kN/mm and 9 kN/mm respectively in the first cycle. As the frequency decreases the storage stiffness decreases. The storage stiffness decreases to approximately 7 kN/mm at the end of the fifth cycle for 1 Hz. For the other frequencies the storage stiffness vanishes.
The loss stiffness has different values between 0.2 Hz and 1 Hz for the first cycle. As the frequency decreases the lost stiffness increases. After the second cycle the loss stiffness remains almost the same and the average value is determined as 56 kN/mm.

The damping coefficient is almost zero between 1.0 Hz-0.7 Hz for the first cycle. For the 0.6, 0.5, 0.4, 0.3 and 0.2 Hz the damping coefficient are 2, 5, 10, 24 and 44 kNs/mm, respectively. After the first cycle the damping coefficient becomes constant and increases as the frequency decreases. The damping coefficients are 8.5 kNs/mm and 46 kNs/mm for 1 Hz and 0.2 Hz respectively.

The equivalent damping ratio is almost zero between 1.0 Hz-0.7 Hz for the first cycle. For the 0.6, 0.5, 0.4, 0.3 and 0.2 Hz the equivalent damping ratio are 0.07, 0.15, 0.23, 0.40 and 0.49 respectively. After the first cycle the equivalent damping ratio becomes constant at approximately 0.50 for each frequency level (Fig. 5.2).

6. CONCLUSIONS

A new LED having some diverse features from the most existing ones in the literature has been designed and produced in this study. The main characteristics of the LED have been determined by conducting the constant frequency altered amplitude and the constant amplitude altered frequency tests.

The characteristics of storage stiffness, loss stiffness and damping coefficients are determined by the computer code relying on the equations given above. There exists an incremental trend for the loss stiffness and damping coefficients between the first and second cycles. The characteristics have not been affected with the increased number of cycles.

In the static tests in which a loading frequency of 0.01667 Hz was used, the dissipated energy is increasing with the increment of displacement intensity. The equivalent damping ratio varies between 20-35% depending on the intensity of the LED displacement.

In the dynamic tests conducted for 2.00 mm displacement, the dissipated energy is less affected with the frequency level. The equivalent damping ratio is attained about 50% for various frequency levels.

It can be concluded that the equivalent damping ratio obtained from the LED is sensitive to displacement intensity and free from the loading frequency in the range of 0.2 Hz and 1.0 Hz.

AKCNOWLEDGEMENT

Funding for this research was provided by ITU Department of Scientific Research Projects (Research Projects 34285, 34014, 35057 and 35065). Researchers are gratefully thankful to the directors and the staff of the STEELAB. The contribution of Irmak Cagdas Makina Industry and Trade Limited Company and Pet-Mak Industry and Trade Limited Company is also gratefully acknowledged.

REFERENCES

Aiken I. (1996). Passive Energy Dissipation-Hardware and Applications. *Proceedings of the Los Angeles County and SEAOSC Symposium on Passive Energy Dissipation Systems for New and Existing Buildings*. Los Angeles.

Birchenall, CE. (1959). Physical Metallurgy, McGraw-Hill, London.

Chopra, AK. (2001). Dynamics of Structures: Theory and Applications to Earthquake Engineering., 2nd Ed., Pearson Prentice Hall, Pearson Education Inc., Upper Saddle River, NJ 07458.

Constantinou, MC. and Symans, MD. (1992). Experimental and Analytical Investigation of Seismic Response of Structures with Supplemental Fluid Viscous Dampers. Technical Report NCEER-92-0032. State University of New York at Buffalo. Department of Civil Engineering. Buffalo, New York.

Cousins, WJ. and Porritt, TE. (1993). Improvements to Lead-Extrusion Damper Technology. *Bulletin of the New Zealand National Society for Earthquake Engineering*. **26(3)**, 342-348.

Robinson, WH. and Greenbank, LR. (1975). Properties of an Extrusion Energy Absorber. *Bulletin of the New Zealand Society for Earthquake Engineering*. **8(3)**, 187-191.

Robinson, WH. and Greenbank, LR. (1976). Extrusion Energy Absorber Suitable for The Protection of Structures During an Earthquake. *Earthquake Engineering & Structural Dynamics*. **4(3)**, 251-259.

Robinson, WH. and Cousins, WJ. (1987). Recent Developments in Lead Dampers for Base Isolation. *Pacific Conference On Earthquake Engineering*. **Vol. 2**. New Zealand.

Rodgers, GW., Chase, JG., Mander, JB., Leach, NC., Denmead, CS., Cleeve, D., Heaton, D. (2006). High Force-to-Volume Extrusion Dampers and Shock Absorbers for Civil İnfrastructure. *19th Australasian Conference on Mechanics of Structures and Materials, Christchurch*. New Zealand.

Rodgers, GW., Chase, JG., Mander, JB., Leach, NC., Denmead, CS. (2006). Experimental Development, Tradeoff Analsis and Design Implemention of High Force-to-Volume Extrusion Damper Technology. *Bulletin of the New Zealand National Society for Earthquake Engineering*. **40(2)**, 35-48.

Rodgers GW. (2009). Next Generation Structural Technologies: Implementing High Force-to-Volume Energy Absorbers, PhD Thesis, University of Canterbury. New Zealand.

Sadek, F., Mohraz, B., Taylor, AW., Chung, RM. (1996). Passive Energy Dissipating Devices for Sesismic Applications. Report NISTIR 5923. Building and Fire Research Laboratory, National Institute of Standarts and Technology, Gaithersburg, Maryland.

Seleemah, AA. and Constantinou, MC. (1997). Investigation of Seismic Response of Buildings with Linear and Nonlinear Fluid Viscous Dampers. Technical Report NCEER-97-0004. State University of New York at Buffalo. Department of Civil Engineering. Buffalo, New York.

Skinner, RI., Robinson, WH., McVerry, GH. (1993). An Introduction to Seismic Isolation, John Wiley and Sons, New York.

Tsai, CS., Lai, WS., Chang, CW., Li, MC. (2002). Testing and Analysis of a New Lead-Extrusion Damper. *Pressure Vessels and Piping Conference*. August 5-9, Vancouver, BC, Canada.

Wulf, J., Taylor, JF., Shaler, AJ. (1956). Metallurgy for Engineers, John Wiley and Sons, New York.